PHYSICAL REVIEW B, VOLUME 64, 060402(R)

History-dependent phenomena in the transverse Ising ferroglass: The free-energy landscape

Ying-Jer Kao,[1] G. S. Grest,[2] K. Levin,[1] J. Brooke,[3] T. F. Rosenbaum,[1] and G. Aeppli[3]
[1]*James Franck Institute and Department of Physics, University of Chicago, Chicago, Illinois 60637*
[2]*Sandia National Laboratory, Albuquerque, New Mexico 87185*
[3]*NEC Research Institute, 4 Independence Way, Princeton, New Jersey 08540*
(Received 15 December 2000; published 3 July 2001)

In this paper we investigate the relationship between glassy and ferromagnetic phases in disordered Ising ferromagnets in the presence of transverse magnetic fields, Γ. Iterative mean-field simulations probe the free-energy landscape and suggest the existence of a glass transition as a function of Γ which is distinct from the Curie temperature. Experimental field-cooled and zero-field-cooled data on $LiHo_xY_{1-x}F_4$ provide support for our theoretical picture. Here as well we present a collection of theoretical predictions for future experiments.

DOI: 10.1103/PhysRevB.64.060402 PACS number(s): 75.50.Lk, 73.43.Nq, 75.10.Nr

The disordered Ising ferromagnet $LiHo_xY_{1-x}F_4$ in a transverse field Γ provides a unique opportunity to study coexistent glassy and ferromagnetic tendencies. Application of Γ tunes both the glassiness and the ferromagnetism and, thereby, makes it possible to probe the complex free-energy landscape. While the glassy characteristics of the paramagnetic transverse Ising systems have been studied both experimentally[1] and theoretically,[2–10] as has the ferromagnetic transition in the pristine system,[11] little is known about the interplay of ferromagnetism and glassiness. Equally interesting is another unique opportunity afforded by the $LiHo_xY_{1-x}F_4$ system, namely the ability to explore quantum mechanical effects arising from $\Gamma \neq 0$, in the presence of glassiness.[12]

The goal of this paper is to study these two coexistent phenomena (glassiness and long range magnetic order) via an exploration of the free-energy surface, and in this way, make systematic predictions for the irreversibility characteristics (i.e., hysteresis, remanent magnetization, etc.). Ferromagnetism in the presence of significant disorder introduces a new class of challenging problems. We show here that the ferromagnetic onset temperature T_c is distinct from the glass transition temperature T_g, and that the latter is itself dependent on the history of the system. Here, in contrast to the rather extensive theoretical studies (of the paramagnetic phase) in the literature,[2–10] we associated T_g, in more physical terms, with the onset of irreversibility in measurable characteristics. In general, there are three state variables, including longitudinal fields, H_z, as well as Γ and T, which can be cycled in many different and noncommuting ways to arrive at a given minimum in the free-energy surfaces.

To support this physical picture, in this paper we also present experimental data showing the difference between field-cooled (FC) and zero-field-cooled (ZFC) magnetic *susceptibilities* as a function of T at fixed Γ in $LiHo_{0.44}Y_{0.56}F_4$. We find that this difference vanishes at a (glass transition) temperature distinct from the Curie point for ferromagnetic ordering.

We base our theoretical analysis on earlier work in conventional spin glasses[13] and random field systems[14] which addressed the evolution of the free-energy landscape using an iterative numerical mean-field scheme, in which the reaction terms (which led to problems with numerical convergence[15]) were ignored. By following a given free-energy minimum as it evolved with field and T, one arrived at rather good agreement between theory and experiment for the various history-dependent magnetizations.

This theoretical approach probes the system on intermediate time scales, which are long compared to the time needed to ''re-equilibrate'' after a given free-energy minimum has disappeared (with temperature or field cycling), but short compared to the time needed to tunnel[1,12] between metastable states on the free-energy surface.

The transverse Ising ferroglass is described by the Hamiltonian:

$$\mathcal{H} = -\frac{1}{2}\sum_{\langle i,j\rangle} J_{ij} S_i^z S_j^z - H_z \sum_i S_i^z - \Gamma \sum_i S_i^x, \qquad (1)$$

where the sum $\langle ij \rangle$ is over the nearest neighbors, and the exchange coupling $J_{i,j}$ is given by the Gaussian distribution $P(J_{ij}) = \sqrt{1/2\pi J^2}\exp(-(J_{ij}-J_0)^2/2J^2)$, where J is the variance and J_0 is the shift. Here $\Gamma \propto H_t^2$ for small H_t, where H_t is the transverse magnetic field applied in the laboratory. We can obtain a mean-field equation for the average magnetization $m_i = \langle S_i^z \rangle_T$ ($\langle \ldots \rangle_T$ denotes thermal averaging) at each site for $S = 1/2$:

$$m_i = \frac{\mathcal{P}_i}{4\mathcal{E}_i}\tanh(\beta \mathcal{E}_i), \qquad (2)$$

where $\mathcal{P}_i = \Sigma_{<i,j>} J_{ij} m_j + H_z$ and $\mathcal{E}_i = \sqrt{\mathcal{P}_i^2 + \Gamma^2}/2$. This mean-field equation corresponds to minimizing the free-energy F as a function of the set of m_i. Here, the transverse field Γ effectively enters only through the modified Brillouin function of Eq. (2), reflecting the fact that Γ rotates the local spin axis away from the Ising or z direction. Introducing this term in effect mixes the ''z-component'' eigenstates of the $\Gamma = 0$ problem. Finally, it should be noted that while the experiments we will present here address the magnetic susceptibility ($\chi = \Sigma \chi_i$ with $\chi_i = \partial m_i / \partial H_z$), the calculations are based on the actual magnetizations. Iterative convergence of the susceptibilities at a given site has not yet been established.

The system in the present study is composed of $N \times N \times N$ spins with random bond configurations. Most of our

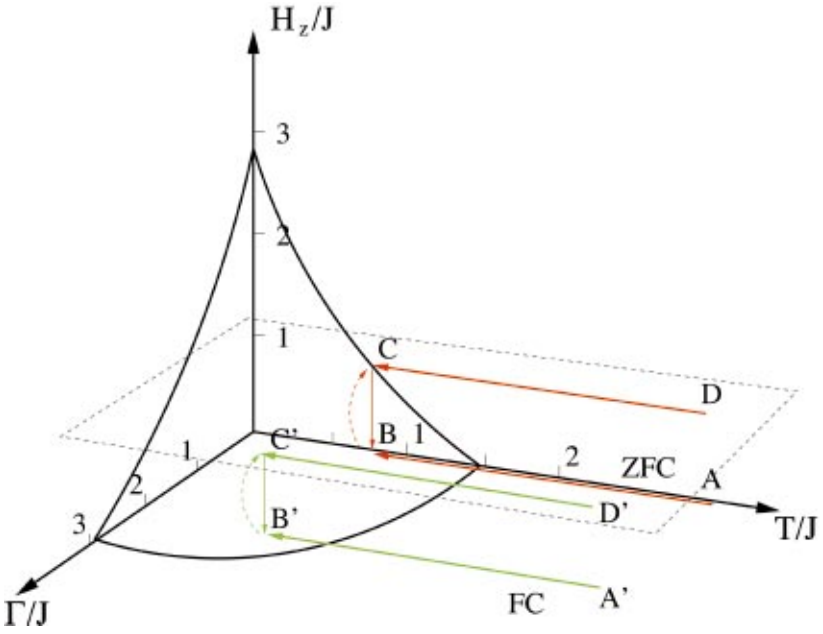

FIG. 1. (Color) Magnetic field and temperature cycling protocols in the parameter space used to tune the free-energy surface. The ZFC state is achieved through cooling from A to B and FC from A' to B'. The remanent magnetizations (called IRM and TRM) are obtained through the paths A-B-C-B, and D-C-B, respectively. The solid lines represent a consolidation of Fig. 5 as discussed in the text below.

examples are for $N=20$ and fixed J_0, although we studied larger ($N=40$) size systems (and variable J_0) to verify convergence of our results. In order to make a closer connection to the experiments,[12] we present here the study of $J_0=0.2J$ so that the system is only slightly ferromagnetic. For each set of parameters (Γ,H_z,T), we start our iterations at the m_i corresponding to the minimum of F evaluated at the previous T,H_z, or Γ. We then update m_i by solving the mean-field equations, Eq. (2), at each site until convergence is obtained at the nth iteration defined by $\Sigma_i(m_i^n-m_i^{n-1})^2/\Sigma_i(m_i^n)^2 \leqslant 10^{-6}$. Unless indicated, the magnetizations discussed in this paper are taken to be along the z (Ising) axis. Finally, a small $H_z=0.01J$, was applied in all studies of glassy properties. This was needed to establish a fixed direction for spontaneous broken symmetry.

Figure 1 is a three-dimensional plot of the parameter space which we consider; these parameters cause the free-energy surface to evolve in distinct ways. Various pathways in this parameter space will be referred to throughout the text. The solid lines shown here are irreversibility contours derived from magnetic hysteresis curves that are discussed later in the paper.

In Fig. 2 we present an $H_z=0$ phase diagram for the Hamiltonian of Eq. (1), omitting the lowest T regime where tunneling effects are important. There are two distinct lines separating different phases: the outer line indicates the phase boundary for the paramagnetic to ferromagnetic phases and the inner line is the ferromagnet to ferroglass phase boundary. The glassy boundary was determined by the condition that the transverse field-cooled (FC) and zero-field-cooled (ZFC) magnetizations are equivalent. The various cooling pathways can be seen in Fig. 1. It should be stressed that in vanishing transverse field the quantity T_g has meaning only as an asymptote, since the distinction between FC and ZFC becomes meaningless when there is no field. The para/ferro boundary is defined by the set of (Γ,T) at which a spontaneous magnetization appears. For a given N, this magnetization may be calibrated by first establishing a baseline zero, which is the magnitude of ''spontaneous magnetization'' due to finite size effects, estimated from the $J_0=0$ case. By changing J_0, we were able to change the position of the para/ferromagnetic line relative to the glassy line; for smaller J_0, the para/ferromagnetic line will be inside the glassy line.

We now turn to experiments. $LiHoF_4$ is a three-dimensional, dipolar-coupled Ising magnet. In the classical limit ($\Gamma=0$), the Ho dipoles order ferromagnetically at a Curie temperature $T_c=1.53$ K. Experiments confirm that standard mean field theory describes fully the critical behavior of the phase boundary between paramagnet and ordered ferromagnet[11]. Moreover, magnetically inert yttrium can be substituted for the holmium spins in single crystals of $LiHo_xY_{1-x}F_4$, permitting carefully controlled studies of the effects of quenched disorder. We suspended a needle of

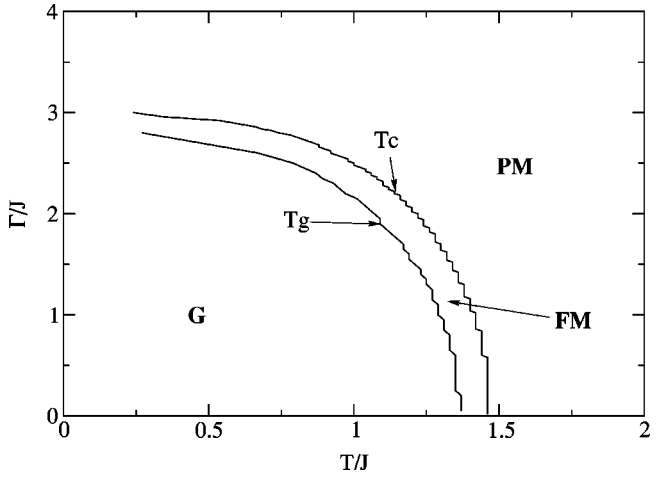

FIG. 2. Mean-field phase diagram of the Ising ferroglass in transverse magnetic field Γ. Here T_g is determined by the point at which the FC and ZFC magnetizations are equal, and, consequently, is defined only for finite Γ.

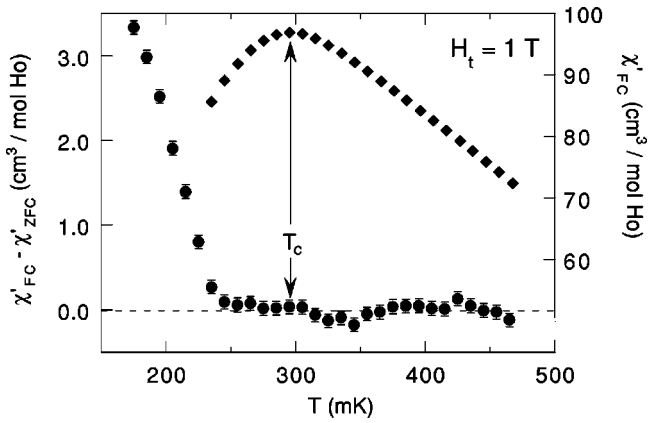

FIG. 3. Temperature evolution of the ac magnetic susceptibility χ' of $LiHo_{0.44}Y_{0.56}F_4$ at $H_t=1$ T for the FC protocol and the difference in χ' under FC and ZFC protocols. The Curie temperature (T_c) in this transverse field is 295 mK while the FC and ZFC susceptibilities bifurcate at $T=240$ mK.

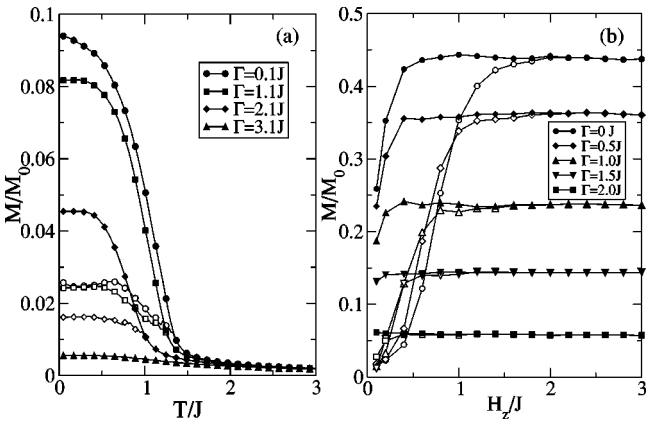

FIG. 4. (a) Temperature dependence of zero-field-cooled (ZFC, open symbols) and field-cooled (FC, closed symbols) magnetizations for the Ising ferroglass at different Γ. (b) Field dependence of IRM (open symbols) and TRM (closed symbols) versus H_z for different Γ at $T=0.15J$.

$LiHo_{0.44}Y_{0.56}F_4$ with $T_c(\Gamma=0)=670$ mK from the mixing chamber of a helium dilution refrigerator into the bore of an 8 T superconducting magnet aligned perpendicular to the Ising c axis (within 0.5°). A trim coil oriented along the Ising axis nulled stray longitudinal fields from the magnets. We measured the ac magnetic susceptibility χ' in the frequency and excitation independent limits using a digital lock-in technique.

We compare in Fig. 3 the system response after various trajectories in H_t-T space, where the static longitudinal field has been carefully set to zero. In the FC protocol, the sample was cooled in $H_t=1$ T from the paramagnet into the ordered state at $T=175$ mK and then warmed; in the ZFC protocol, H_t was only applied after cooling to 175 mK. The ferromagnetic transition is marked by a peak in field-cooled susceptibility at $T=295$ mK. By contrast, the FC and ZFC susceptibilities bifurcate deeper in the ordered state, at $T=240$ mK. As is consistent with the theoretical mean-field phase diagram of Fig. 2, we find clearly distinct signatures for ferromagnetism and glassiness in the disordered Ising magnet $LiHo_{0.44}Y_{0.56}F_4$.

To elucidate these data, FC and ZFC processes were simulated numerically as in classical spin glasses,[13] with the fields applied in the transverse direction. We first cooled down the system in zero external field (path $A\rightarrow B$ in Fig. 1). We then applied a transverse field, and warmed up the system. In this way we obtained a zero-field-cooled magnetization M^{ZFC} as a function of temperature. These results are shown by the open symbols in Fig. 4(a). We next cooled the system in the presence of a transverse field to $T=0.1J$ (path $A'\rightarrow B'$) and then warmed up in the presence of this field. We thereby obtained the M^{FC} curve [indicated by the solid symbols in Fig. 4(a)]. The two magnetizations merge at a given temperature T_g, which we identify as the glass transition temperature of Fig. 2. We found that M^{FC} is reversible upon cooling and warming, while M^{ZFC} is not reversible for a subsequent cooling from a temperature lower than T_g. In this way we can regard the FC state as that which is closer to true thermodynamical equilibrium, and it should not be surprising that this state has the larger magnetization of the two; this larger M takes advantage of the net ferromagnetic bias J_0. As the system is warmed the magnetization decreases monotonically. For both M^{FC} and M^{ZFC}, the magnetizations at the lowest temperatures decrease as Γ increases. This is a consequence of the off-diagonal components introduced by Γ, which act to reduce the net magnetization in the z direction.

We turn now to the issue of remanent magnetizations. These remanences arise following the removal of a magnetic field, when the system becomes trapped in a metastable minimum. In canonical Ising spin glasses there are two characteristic remanences[13] (associated with H_z). These are the isothermal remanent magnetization (IRM) and the thermal remanent magnetization (TRM). In the presence of a *fixed* transverse field we modify their definitions slightly, as follows. We first consider the case $\Gamma=0$. When the system is cooled through path $A\rightarrow B$ in Fig. 1 and a longitudinal field is applied instantaneously ($B\rightarrow C$) and subsequently adiabatically removed ($C\rightarrow B$), we refer to the resulting magnetization as the thermal remanent magnetization. When the system is cooled through path $D\rightarrow C$ in a longitudinal field and the field is adiabatically turned off ($C\rightarrow B$), we refer to the resulting magnetization as the isothermal remanent magnetization. For the present purposes we will be interested in the IRM and TRM at finite Γ. This corresponds to the paths $A'\rightarrow B'\rightarrow C'\rightarrow B'$ and $D'\rightarrow B'\rightarrow C'$, respectively. The behavior of the two remanences at different Γ is shown in Fig. 4(b) for $T=0.15J$. Both the TRM (closed symbols) and the IRM (open symbols) become smaller as Γ increases, as expected since the spins are aligned more toward the transverse field direction. We find that the H_z value where the two remanences are equal becomes smaller as Γ increases, indicating that at higher Γ it takes less H_z to destroy the multiple minima on the free-energy surface.

As a final protocol, we address the behavior of magnetic hysteresis loops (for the magnetization as a function of varying H_z), in the presence of fixed transverse fields. The results are shown in Figs. 5(a)–(d), where the transverse fields are

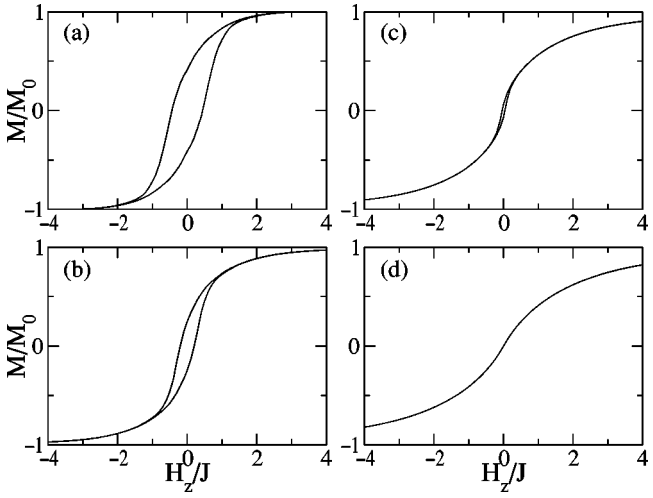

FIG. 5. Hysteresis loops at fixed $\Gamma =$ (a) $0.0J$, (b) $1.0J$, (c) $2.0J$, and (d) $3.0J$. Here $T=0.15J$.

$\Gamma=0.0J$, $1.0J$, $2.0J$, and $3.0J$, respectively. The loops were obtained by slowly decreasing the parallel field (H_z) from the high field limit ($4J$) until an equally large negative field was reached and then sweeping back to close the loop. As is evident, a nonzero transverse field enables the hysteresis loop to close at smaller H_z.

We may summarize these numerical hysteresis studies in a three-dimensional plot of the associated irreversibility surface (solid lines in Fig. 1). The surface consists of the locus of points in terms of the coordinates (Γ,H_z,T) below which the system exhibits irreversibility, as reflected in magnetic hysteresis loops. It should be stressed that this protocol is different from that used to obtain T_g in Fig. 1. While both protocols are experimentally accessible, the point at which irreversibility sets in for a given (Γ,H_z,T) is not unique, and, itself, depends upon the pathway to the point in question. This scenario is to be distinguished from the more conventional situation which in either Γ or H_z is strictly set to zero, as in Refs. 13 and Refs. 2–10, respectively. An important conclusion from Fig. 1 is that raising the temperature or applying a longitudinal or transverse magnetic field progressively removes minima from the free-energy surface until at sufficiently high temperatures or fields there is a unique state.

The calculations which underlie this figure ignore thermal, as well as quantum, fluctuations. Given the latter, the low temperature regime should be viewed as inaccessible. Our results can be contrasted with a recent low temperature study (in the paramagnetic phase) which investigated the glassy phase in a quantum *p*-spin spherical model within an equilibrium statistical mechanical approach.[16] Here it was observed that hysteretic effects may also arise from a first-order phase transition, rather than from the glassiness which we have emphasized here. It should be noted that the experimental hysteresis reported in Fig. 3 is not strictly in the quantum regime. However, to make a firm distinction between these two theoretical scenarios will require further experiments.

In summary, in this paper we have emphasized the concept of history-dependent measurements in transverse Ising ferroglasses, a concept that has been widely recognized in other magnetic glasses.[17] Because of its focus on the complex free-energy landscape, our approach should be contrasted with alternatives in the literature, which have also addressed the phase diagram of $LiHo_xY_{1-x}F_4$, but with an emphasis on the low temperature quantum regime using equilibrium statistical mechanics. It should also be stressed that these transverse field configurations represent a unique opportunity to simultaneously tune glassiness along with long range ferromagnetic order. Our predictions for the *intermediate time scale* behavior of the various history-dependent magnetizations appear consistent with the FC and ZFC susceptibility measurements presented here, but further experiments will be needed to confirm the set of predictions presented here.

We thank Qimiao Si for useful conversations. The work at the University of Chicago was supported by the NSF-MRSEC, under Grant No. DMR-9808595. Sandia is a multiprogram laboratory operated by Sandia Corporation, a Lockheed Martin Company, for the United States Department of Energy under Contract DE-AC04-94AL85000.

[1] G. Aeppli and T. F. Rosenbaum, in *Dynamical Properties of Unconventional Magnetic Systems*, edited by A. T. Skjeltorp and D. Sherrington (Kluwer Academic Publishers, Netherlands, 1998), pp. 107–122.

[2] K. Walasek and K. Lukierska-Walasek, Phys. Rev. B **34**, 4962 (1986); **38**, 725 (1988).

[3] T. K. Kopeć, J. Phys. C **21**, 297 (1988).

[4] P. Ray, B. K. Chakrabarti, and A. Chakrabarti, Phys. Rev. B **39**, 11 828 (1989).

[5] H. Ishii and T. Yamamoto, J. Phys. C **18**, 6225 (1985).

[6] Y. Y. Goldschmidt and P.-Y. Lai, Phys. Rev. Lett. **64**, 2467 (1990).

[7] G. Büttner and K. D. Usadel, Phys. Rev. B **41**, 428 (1990).

[8] R. R. dos Santos, R. Z. dos Santos, and M. Kischinhevsky, Phys. Rev. B **31**, 4694 (1985).

[9] H. Rieger and A. P. Young, Phys. Rev. Lett. **72**, 4141 (1994).

[10] M. Guo, R. N. Bhatt, and D. A. Huse, Phys. Rev. Lett. **72**, 4137 (1994).

[11] D. Bitko, T. F. Rosenbaum, and G. Aeppli, Phys. Rev. Lett. **77**, 940 (1996).

[12] J. Brooke, D. Bitko, T. F. Rosenbaum, and G. Aeppli, Science **284**, 779 (1999).

[13] C. M. Soukoulis, K. Levin, and G. S. Grest, Phys. Rev. Lett. **48**, 1756 (1982); C. M. Soukoulis, K. Levin, and G. S. Grest, Phys. Rev. B **28**, 1495 (1983).

[14] C. Ro *et al.*, Phys. Rev. B **31**, 1682 (1985).

[15] D. D. Ling, D. R. Bowman, and K. Levin, Phys. Rev. B **28**, 262 (1982).

[16] L. F. Cugliandolo, D. R. Grempel, and C. A. da Silva Santos, Phys. Rev. Lett. **85**, 2589 (2000).

[17] R. J. Birgeneau, J. Magn. Magn. Mater. **177**, 1 (1998).